

Laboratori Nazionali di Frascati

LNF-68/9

C. Bacci et al. : ANGULAR DISTRIBUTION FOR ETA-MESON
PHOTOPRODUCTION FROM HYDROGEN AT 775-850 MeV.

Estratto da : Phys. Rev. Letters 20, 571 (1968)

**ANGULAR DISTRIBUTION FOR ETA-MESON PHOTOPRODUCTION
FROM HYDROGEN AT 775-850 MeV**

C. Bacci

Istituto Nazionale di Fisica Nucleare, Sezione di Roma, Roma, Italy

and

R. Baldini-Celio, C. Mencuccini, A. Reale, M. Spinetti, and A. Zallo

Laboratori Nazionali di Frascati del Comitato Nazionale per l'Energia Nucleare, Frascati, Italy

(Received 3 January 1968)

In this paper we report an experiment performed at the Frascati 1.1-GeV electron synchrotron on the photoproduction of the eta meson from hydrogen,

$$\gamma + p \rightarrow \eta + p. \quad (1)$$

The forward differential cross section has been measured at the three energies $K = 775$, 800 , and 850 MeV of the incident photons for different eta c.m. angles θ_η^* . The energy resolution ΔK was typically ± 25 MeV. The purpose of

this experiment was to investigate, not far from threshold energy, the presence in photoproduction of higher partial waves besides the dominant η -nucleon S-wave resonance.¹

Our results show that in the reaction $\gamma + p \rightarrow \eta + p$ up to $K = 850$ MeV (corresponding to a c.m. total energy $E^* = 1573$ MeV), the differential cross section is not sensibly increasing at forward angles. At backward angles a departure from isotropy could start between $K = 800$ MeV and $K = 850$ MeV. At the correspond-

ing c.m. total energies, the angular distributions for the reaction^{2,3} $\pi^- + p \rightarrow \eta + n$ are clearly not isotropic.

The experimental setup is shown in Fig. 1. The γ -ray beam was incident on a cylindrical liquid-hydrogen target 7 cm in diameter and was monitored by a Wilson-type quantameter.⁴ The η 's from Reaction (1) were detected by measuring both the angles and energies of their two decay photons. Each photon detector was a lead-glass total-absorption Cherenkov counter with a veto scintillation counter in front, covering a typical laboratory solid angle of 12 msr.

Two pairs of photon detectors were permanently used in order to increase the collection rate and to reduce possible sources of systematic instrumental errors.

For each pair of photon detectors, events giving a coincidence ($C_1 C_2 \bar{S}_1 \bar{S}_2$ or $C_3 C_4 \bar{S}_3 \bar{S}_4$) were recorded and the corresponding pulse heights from the Cherenkov registered and analyzed using a PDP8 computer on line. Systematic calibrations with monochromatic electrons from a pair spectrometer were made. The

gain stability in the pulse-height analysis was automatically controlled⁵ during the measurement. The energy resolution of our photon detectors was about $\pm 16\%$ at 500 MeV, changing roughly as $E^{-1/2}$ with the photon energy. The kinematical definition of the events from Reaction (1) depends on the opening angle 2β between the photon detectors and the maximum energy of the bremsstrahlung spectrum. In fact, the kinematics of $\eta - \gamma + \gamma$ gives a minimum angle between the two γ 's which increases as the η energy decreases; so the minimum energy for detectable η is determined by the maximum angle covered by the photon detectors. On the other end, the maximum η energy is fixed essentially by the maximum energy of the bremsstrahlung spectrum. For each of the kinematical situations considered, the events are represented by points in a two-dimensional logarithmic plot whose coordinates are the energies of the two detected photons [Figs. 2(a) and 2(b)]. In this plot the η events from Reaction (1) are expected to occupy a well-defined region which has been determined by a Monte Carlo calculation taking properly into account the measured energy resolution of the Cherenkov and the geometrical situation.

Concerning the background, the single- π^0 photoproduction process is completely ruled out for kinematical reasons since a bias of $E_\gamma \approx 100$ MeV in the photon energy is set in each Cherenkov counter. The background of $\gamma\gamma$ events showing up outside the η region [in Fig. 2(a)] is mainly due to multiple π^0 production and other η decays. For this background, strong correlation between the energies of the two detected photons is not expected. Thus, to measure this contamination the geometry was slightly changed in order to exclude the η -event detection, but at the same time keeping constant the angle of each Cherenkov counter with respect to the γ -ray beam line. With this procedure we have found that the background counting rate outside the η region did not change. A typical background spectrum is shown in Fig. 2(b).

By projecting the η events of the $E_{\gamma_1}, E_{\gamma_2}$ plot on the bisector of the coordinates, after having subtracted the background, a mass histogram is derived which is shown in Fig. 2(c). The solid line represents the mass distribution for the $\eta - \gamma + \gamma$ decays as predicted by a Monte Carlo calculation.

Our results on the differential cross section

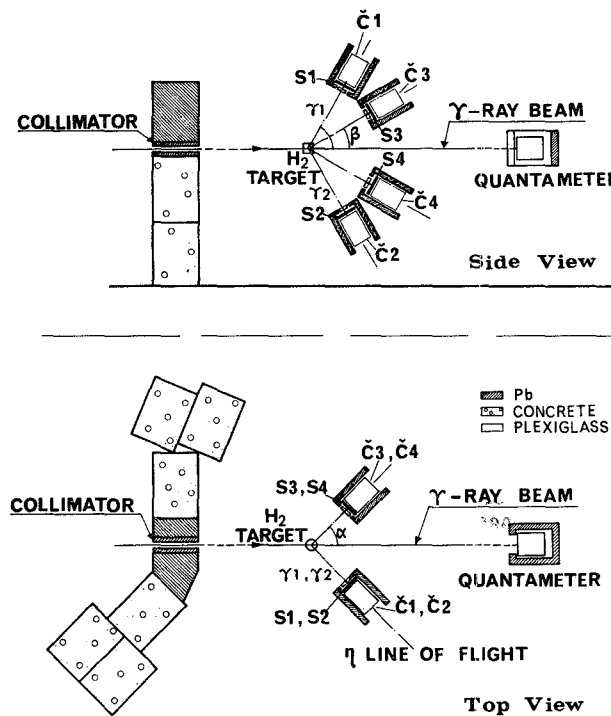


FIG. 1. Experimental setup for the two pairs of photon detectors. The angle α is the laboratory emission angle of the η , while 2β represents the opening angle of the two detected γ 's from the decay $\eta \rightarrow \gamma + \gamma$. C_1, C_2 and C_3, C_4 are lead-glass Cherenkov counters; S_1, S_2 and S_3, S_4 , veto scintillation counters.

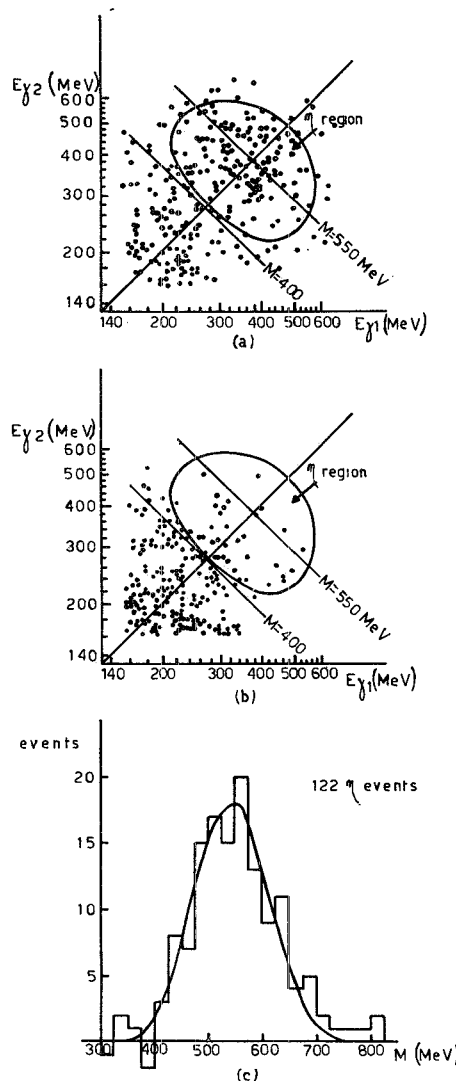


FIG. 2. (a) Typical $E_{\gamma_1}, E_{\gamma_2}$ plot when the η detection is allowed by the geometrical arrangement of the Cherenkov counters; the dotted line which defines the η region is calculated by a Monte Carlo program. The full lines $M = \text{const}$ represent the loci of $\gamma\gamma$ events from 2γ decays of particles of masses M in case of point counters. (b) The same as (a) but with the η not detectable because of the opening angle of the photon detectors. (c) Mass histogram as obtained by projecting the $\eta \rightarrow \gamma + \gamma$ events of (a) on the bisector of the coordinates after having subtracted the background. The full line gives the η peak shape as predicted by a Monte Carlo calculation.

for η photoproduction in hydrogen are shown in Fig. 3.

The measured c.m. cross sections $(d\sigma/d\Omega^*)_{\gamma\gamma}$ for Reaction (1) when the η decays by the $\eta \rightarrow \gamma + \gamma$ mode are reported on the ordinates on the left-hand side of Fig. 3. The differential cross sections $(d\sigma/d\Omega^*)_{\text{all modes}}$ for all the decay modes

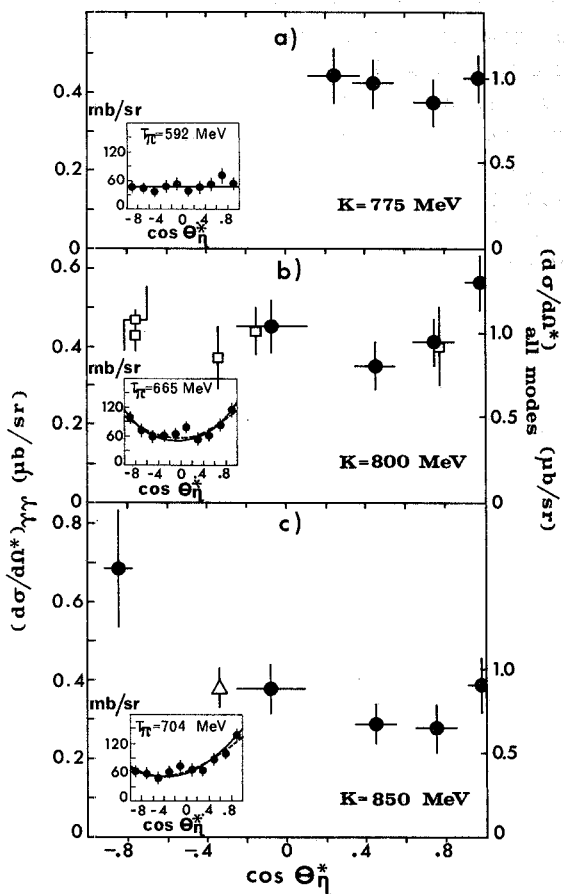


FIG. 3. Experimental results $d\sigma(\eta \rightarrow \gamma + \gamma)/d\Omega^*$ (ordinates on the left-hand side) and $d\sigma(\eta \rightarrow \text{all modes})/d\Omega^*$ (ordinates on the right-hand side) as a function of θ_{η^*} (c.m. angle of the η) at the three different energies K of the incident photon. The points indicated with open squares in (b) are from Ref. 7. The point indicated with an open triangle in (c) is from Ref. 8. The angular distribution results (Ref. 2) for the reaction $\pi^- + p \rightarrow \eta + n$ at approximately the same c.m. total energy are reported in the small frames.

of the produced η are reported on the ordinates on the right-hand side in Fig. 3 as calculated from $(d\sigma/d\Omega^*)_{\gamma\gamma}$ by using the last world average⁶ for $\Gamma(\eta \rightarrow \text{all modes})/\Gamma(\eta \rightarrow \gamma + \gamma) = 1/0.43 = 2.32$.

The errors we quote in Fig. 3 are inclusive of the uncertainties on the background subtraction. In addition, there are systematic errors due to the uncertainties on the quantameter calibration, target thickness, shape of the bremsstrahlung spectrum near the maximum energy, and efficiency calculation, which we estimate to yield an over-all systematic error of $\approx \pm 10\%$ (not included in Fig. 3). Our experimental points in Fig. 3 show as horizontal flags

the angular interval over which the cross section is averaged.

In Fig. 3 previous experimental results^{7,8} on η photoproduction are also reported.

The data we report suggest the following remarks:

(a) The data points at 775 and 800 MeV show an angular distribution essentially isotropic. At $K=850$ MeV the forward angular distribution is still consistent with isotropy, while the point we have measured at $\theta_{\eta^*}=150^\circ$ could represent a tendency to an increase of the cross section at backward angles. In this respect an extension of this measurement in the backward region could be interesting. At $K=850$ MeV a best fit to the experimental points with a $\cos\theta_{\eta^*}$ polynomial form

$$(d\sigma/d\Omega^*)_{\gamma\gamma} = \sum_{l=0}^N c_l (\cos\theta_{\eta^*})^l$$

gives $\chi^2/n=2.06$ if we put $N=0$ (n is the number of data points minus the number of varied parameters), while we get $\chi^2/n=0.31$ if we let l go up to $N=2$ (in this latter case the following values, in $\mu b/\text{sr}$, are found for the coefficients: $C_0=0.33 \pm 0.03$, $C_1=-0.23 \pm 0.05$, and $C_2=0.25 \pm 0.06$).

(b) The angular distributions for the reaction² $\pi^- + p \rightarrow \eta + n$ at the same c.m. total energy are also reported in the small frames of Fig. 3. A comparison with our results on Reaction (1) shows a rather different behavior of these two reactions. In the $\pi^- + p \rightarrow \eta + n$ angular distributions, terms through $\cos^2\theta_{\eta^*}$ become important already at $T_\pi=655$ MeV. This energy corresponds to $K=800$ MeV for the photoproduction reaction where the distribution is still isotropic. Therefore, in photoproduction on protons, at least up to this energy, no evidence is found of the contributions of P_{11} , D_{13} , or P_{13} partial waves which can explain the $\pi^- + p \rightarrow \eta + n$ angular distribution data.

(c) A possible explanation for the different angular behavior between the reactions $\pi^- + p$

$\rightarrow \eta + n$ and $\gamma + p \rightarrow \eta + p$ might be found by considering that the photoproduction on protons of pure $T=\frac{1}{2}$ isospin states proceeds via combination of both an isoscalar $T^{(0)}$ and an isovector $T^{(1/2)}$ parts in the production amplitude $\langle \eta p | \times T | \gamma p \rangle \propto T^{(0)} - T^{(1/2)}$. It might happen that the two contributions are of the same order of magnitude so that a cancellation is effective and the contribution of some higher partial wave is depressed. If this is the case, the effect of partial waves higher than S_{11} could show itself when the photoproduction occurs on neutrons, since now the contributions of the isoscalar and isovector parts add together: $\langle \eta n | \times T | \gamma n \rangle \propto T^{(0)} + T^{(1/2)}$. In this respect a study of the reaction $\gamma + n \rightarrow \eta + n$ on deuterium would be of interest.

We wish to thank Professor G. Salvini for his critical remarks, suggestions, and continuous interest. The synchrotron staff is thanked for the smooth running of the machine during all the measurement. We deeply thank V. Bidoli and I. Bruno for their contribution in setting up the apparatus and their continuous assistance during the experiment.

¹For a detailed bibliography on this argument we refer to the article of S. R. Deans and W. G. Holladay, Phys. Rev. 161, 1466 (1967).

²W. Bruce Richards, C. B. Chiu, R. D. Eandi, A. C. Helmholz, R. W. Kenney, N. J. Moyer, J. A. Poirier, R. J. Cence, V. Z. Peterson, N. K. Sehgal, and V. J. Stenger, Phys. Rev. Letters 16, 1221 (1966).

³S. Buniyatov, E. Zavattini, W. Deinet, H. Müller, D. Schmitt, and H. Standenmaier, in Proceedings of the International Conference on High-Energy Physics, Heidelberg, Germany, September, 1967 (to be published).

⁴R. R. Wilson, Nucl. Instr. Methods 1, 101 (1957).

⁵C. Bacci, R. Baldini-Celio, and V. Bidoli, Nucl. Instr. Methods 57, 100 (1967).

⁶I. Butterworth, in Proceedings of the International Conference on Elementary Particles, Heidelberg, Germany, 1967 (to be published).

⁷R. Prepost, D. Lundquist, and D. Quinn, Phys. Rev. Letters 18, 82 (1967).

⁸C. Bacci, G. Penso, G. Salvini, C. Mencuccini, and V. Silverstrini, Nuovo Cimento 45A, 983 (1966).